

**SPECTROSCOPIC INVESTIGATION OF CHLORIDE SALT DEPOSITS IN NOACHIS TERRA.** B. P. Phillips<sup>1</sup>, T. D. Glotch<sup>1</sup>, A. D. Rogers<sup>1</sup>, M. M. Osterloo<sup>2</sup>, <sup>1</sup>Department of Geosciences, Stony Brook University, Stony Brook, NY, 11794–2100 (brooke.phillips@stonybrook.edu), <sup>2</sup>Laboratory for Atmospheric and Space Physics.

**Introduction:** Numerous chloride-bearing deposits on Mars have been detected using data from the Mars Odyssey Thermal Emission Imaging System (THEMIS) [1, 2, 3, 4]. The deposits exhibit relatively featureless red spectral slopes in the visible near infrared (VNIR) and blue slopes superimposed on typical basaltic regolith spectral characteristics in the mid-infrared (MIR), consistent with a mixture of anhydrous chlorides and silicates [1, 2]. In terrestrial settings, chloride deposits are associated with other alteration or evaporite phases, such as phyllosilicates and sulfates [4]. On Mars, however, additional evaporites have yet to be detected in association with the chloride deposits [3] and only a few occurrences of coexisting phyllosilicate and chloride salt deposits have been detected [1, 2, 6].

Prior to this work, very few comprehensive studies have attempted to characterize the compositional stratigraphy of the salt deposits in the Noachis Terra region [5]. The objective of this study is to take advantage of multiple orbital datasets (THEMIS, CRISM) at varying spatial and spectral resolution in order to gain insight into the timing and duration of aqueous processes as recorded in the mineralogy of the Noachis Terra region. In particular, we focus here on using a radiative transfer model, principal components analysis, and spectral unmixing methods to identify major mineral components within aqueous mineral deposits in the study region.

**Datasets and Methods:** THEMIS decorrelation stretch (DCS) and CRISM MSP and FRT images were

used to locate units of interest within the study region. CRISM multispectral survey (MSP) maps were used to identify the presence of hydrated minerals, interpreted to be Fe- and/or Mg-rich phyllosilicates, within the study region (Figure 1a). The MSP maps are rendered using the revised CRISM summary products D2300, D2200, BD1900 (as red/green/blue) described by [7]. Compared to higher spatial/spectral resolution CRISM FRT images, accurate surface interpretation using CRISM MSP images (55 wavelength channels; 200 m/pixel spatial resolution) is more challenging due to subpixel intimate and checkerboard mixing [8]. Nevertheless, the CRISM multispectral mapping mode is still a powerful tool for understanding regional-scale compositional variations over various geologic terrains, as well as filling in the data gaps that exist between targeted observations.

CRISM full resolution targeted (FRT) data covers 544 wavelength channels from 0.36–3.92  $\mu\text{m}$  and has a spatial resolution of 18 m/pixel. In this study, CRISM I/F image FRT00009ACE (yellow box in Figure 1b) was atmospherically corrected for both gases and aerosols using the Discrete Ordinate Radiative Transfer model (DISORT) using the method of [8]. Single scattering albedo (SSA) values were acquired under the assumption that surface scattering can be modeled using a Hapke bidirectional reflectance distribution function (BRDF) [9]. The derived single scattering albedos were converted back into radiance coefficients comparable to

laboratory spectra [8] assuming incidence and emergence angles of 30° and 0°, respectively. Through the use of a statistical principal-component approach, known as factor analysis and target transformation (FATT) [10], CRISM spectral end-members were identified from the DISORT-corrected radiance coefficient data for FRT00009ACE. Factor analysis reveals end-members from a spectral image cube as eigenvectors with associated eigenvalues, indicating their relative contribution to the scene. The eigenvectors were then fit to laboratory spectra (target transformation) using a linear least-

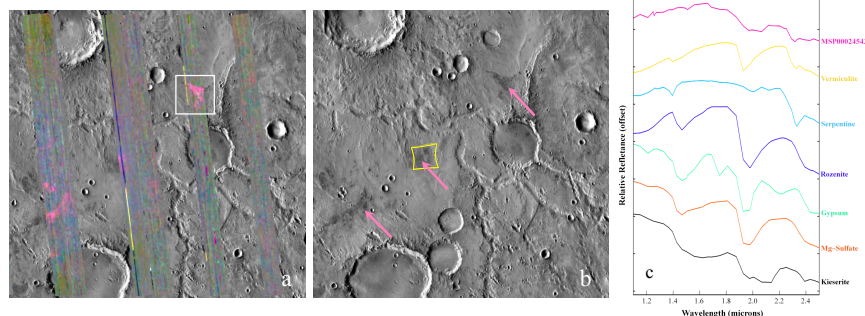


**Figure 1.** (a) CRISM MSP maps displayed over THEMIS daytime IR mosaic. The maps are rendered with CRISM D2300, D2200, and BD1900 summary parameters [7] as red/green/blue, respectively. Hydrated Fe/Mg-phyllosilicates appear magenta. (b) Magenta arrows show the correlation between the Fe/Mg-phyllosilicates and underlying dark material shown in THEMIS daytime IR. The location of CRISM image FRT00009ACE is outlined in yellow. (c) Mean reflectance spectrum collected from identified hydrated material in MSP00024543 (location within white box in 1a) with resampled laboratory spectra of various phyllosilicates and sulfates.

squares model [8, 11]. Best-fit models are considered to be the likely mineralogical components in the scene.

**Results:** Figure 1 shows CRISM MSP index composites over the chosen study area (centered at 353.9°E and -5.69°N). The hydrated phyllosilicates appear magenta and correlate with the underlying darker and thermophysically distinct material observed in THEMIS

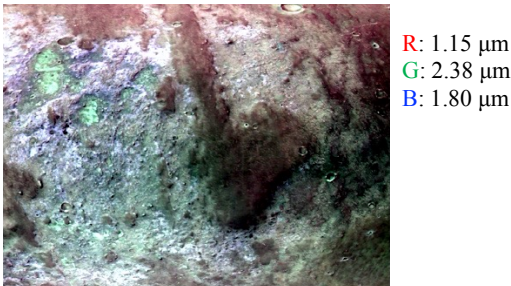


**Figure 2.** RGB image of FRT00009ACE, highlighting regions of spectral interest. Phyllosilicates appear light purple and the chloride deposits are bright cyan/green.

daytime infrared data (Figure 1b). Spectra were collected from a patch of hydrated minerals detected within MSP00024543 (location shown in Figure 1a). The mean reflectance spectrum from this spectrally distinct region is shown in Figure 1c and is best matched with hydrated phyllosilicates. The reflectance data shows absorption features at  $\sim 1.4\mu\text{m}$  due to the O-H stretch overtone,  $1.9\mu\text{m}$  due to a combination of the O-H stretch and H-O-H bending overtones, and a  $\sim 2.2\text{--}2.4\mu\text{m}$  feature that will vary based on the relative abundance of metal-OH bonds within an observed phyllosilicate structure [7]. The  $2\mu\text{m}$  feature observed may be due to residual  $\text{CO}_2$  from the atmosphere [12].

**CRISM Spectral End-Members:** A composite image using three wavelengths ( $1.15$ ,  $2.38$ , and  $1.80\mu\text{m}$ ) from the DISORT-corrected reflectance data from FRT00009ACE (Figure 2) reveals compositional diversity within the scene and allows for the user to choose individual geologic units for spectral unmixing. The linear least squares models utilized laboratory spectra from CRISM spectral libraries. Additional spectral data was collected by [2] for various mixtures of halite (NaCl), labradorite, and flood basalt in order to simulate the spectral signatures of the ratioed CRISM I/F for the FRT00009ACE chlorides. Jensen and Glotch [2], along with a later study completed by [13], concluded that the featureless red slope in the NIR was represented best by a mixture consisting of 10–25% halite with particle size fraction of  $63\text{--}80\mu\text{m}$  [2, 13]. The preliminary FATT-retrieved end-members are shown in Figure 3. As expected from the initial MSP observations, a phyllosilicate component,

most likely vermiculite, is present in the scene. However, a comparison of the chloride-bearing regions to the data collected of the various halite mixtures by [2] do not fully agree with the suggestions made by [2, 13]. Figure 3b shows the best fit models for the various halite/flood basalt mixtures. The chloride-bearing regions within the study area exhibit variable spectral features between  $2.1\text{--}2.5\mu\text{m}$  when compared to the featureless red spectral slope of the halite/flood basalt mixtures collected by [2]. Other best fit components identified were rozenite and Mg-sulfate. These results highlight the complex nature of the light-toned, spectrally featureless materials identified throughout the southern highlands.

**Discussion and Future Work:** Detailed spectroscopic investigations at both regional and local scales will increase our understanding of the compositional diversity and stratigraphic relations of the Noachis Terra chloride deposits to other alteration mineral phases. Future work will focus on detailed geologic mapping of Noachis Terra salt deposits, using a combination of compositional, thermophysical, and geomorphological observations. Absolute model ages will be determined using crater-age dating and will be used to better constrain the timeline of aqueous alteration.

**References:** [1] Osterloo, M. M. et al. (2010) JGR, 115. [2] Jensen, H. B. and Glotch, T. D. (2011) JGR, 116. [3] Murchie, S. L. et al. (2009) JGR, 114. [4] Glotch, T. D. (2010), GRL, 37. [5] Osterloo, M.M. and Hynek, B.M. (2015), Geology, 43, 787–790. [6] Ruesch, O. et al. (2012), JGR, 117, E00J13. [7] Viviano-Beck, C. E. et al. (2014) JGR, 119, 1403–1431. [8] Liu, Y. et al. (2016) JGR, 121, 2004–2036. [9] Hapke, B. (2012) Cambridge Univ. Press. [10] Bandfield, J.L. et al. (2000) JGR, 105. [11] Ramsey M. S. and Christensen P. R. (1998), JGR, 103, 577–596. [12] Amador, E.S. and Bandfield, J.L.(2016), Icarus, 276, 39–51. [13] Glotch, T.D. et al. (2016) JGR, 121.

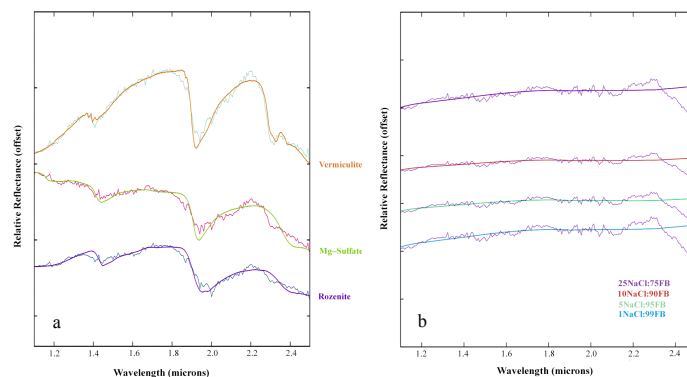


**Figure 3.** (a) Best fit linear least squares models of retrieved eigenvectors and laboratory spectra. FATT results suggest the presence of vermiculite, rozenite, and Mg-sulfate. (b) Model results for halite/flood basalt (FB) mixtures at  $63\text{--}80\mu\text{m}$  size fractions [2] exhibit differing spectral features between  $2.1\text{--}2.5\mu\text{m}$ .